

Effects of Tobacco Smoke on Gene Expression and Cellular Pathways in a Cellular Model of Oral Leukoplakia

Zeynep H. Gümüş,^{1,4} Baoheng Du,² Ashutosh Kacker,³ Jay O. Boyle,⁵ Jennifer M. Bocker,^{2,5} Piali Mukherjee,⁴ Kotha Subbaramaiah,² Andrew J. Dannenberg² and Harel Weinstein^{1,4}

Abstract

In addition to being causally linked to the formation of multiple tumor types, tobacco use has been associated with decreased efficacy of anticancer treatment and reduced survival time. A detailed understanding of the cellular mechanisms that are affected by tobacco smoke (TS) should facilitate the development of improved preventive and therapeutic strategies. We have investigated the effects of a TS extract on the transcriptome of MSK-Leuk1 cells, a cellular model of oral leukoplakia. Using Affymetrix HGU133 Plus 2 arrays, 411 differentially expressed probe sets were identified. The observed transcriptome changes were grouped according to functional information and translated into molecular interaction network maps and signaling pathways. Pathways related to cellular proliferation, inflammation, apoptosis, and tissue injury seemed to be perturbed. Analysis of networks connecting the affected genes identified specific modulated molecular interactions, hubs, and key transcription regulators. Thus, TS was found to induce several epidermal growth factor receptor (EGFR) ligands forming an EGFR-centered molecular interaction network, as well as several aryl hydrocarbon receptor-dependent genes, including the xenobiotic metabolizing enzymes CYP1A1 and CYP1B1. Notably, the latter findings *in vitro* are consistent with our parallel finding that CYP1A1 and CYP1B1 levels were increased in oral mucosa of smokers. Collectively, these results offer insights into the mechanisms underlying the procarcinogenic effects of TS and raise the possibility that inhibitors of EGFR or aryl hydrocarbon receptor signaling will prevent or delay the development of TS-related tumors. Moreover, the inductive effects of TS on xenobiotic metabolizing enzymes may help explain the reduced efficacy of chemotherapy, and suggest targets for chemopreventive agents in smokers.

Tobacco use is an important risk factor for multiple human malignancies and accounts for ~30% of all cancer-related deaths in the United States (1). Exposure to tobacco has been linked to a variety of malignancies including cancers of the lung, oral cavity and pharynx, esophagus, pancreas, liver, bladder, and cervix (2). More than 100 carcinogens, mutagens, and tumor promoters have been identified in tobacco smoke (TS; refs. 3, 4). In addition to being a major cause of cancer,

smoking can alter the activity of chemopreventive agents (4, 5), stimulate the metabolic clearance of targeted anticancer therapies (6), and increase the risk of second primary tumors (7). Although cessation of tobacco use is highly desirable, it is not realistic for everyone. Hence, there is a significant interest in chemopreventive agents that could protect against the carcinogenic effects of TS. Moreover, a clearer understanding of the mechanisms that are modulated by TS should lead to more effective treatments resulting in an improved outcome for cancer patients.

Given the significance of TS as both a cause of cancer and a potential modifier of treatment outcome (1, 8–10), we have investigated the effects of a TS extract on the transcriptome in a cellular model of oral leukoplakia. This model was chosen because the link between exposure to TS and head and neck squamous cell carcinoma is well established. Furthermore, smoking reduces the likelihood of treatment response in head and neck cancer patients (11) and increases the risk of second primary tumors in patients who have been successfully treated for their index head and neck malignancy (7). The transcriptome analysis involved the identification of genes differentially expressed due to TS exposure in this cell line, followed by a classification of these genes into domains of putative physiologic function. The classification involved the

Authors' Affiliations: ¹Physiology and Biophysics, ²Medicine, and ³Otolaryngology, and ⁴HRH Prince Alwaleed Bin Talal Bin Abdulaziz Alsaud Institute for Computational Biomedicine, Weill Medical College of Cornell University; and ⁵Department of Surgery (Head and Neck Service), Memorial Sloan-Kettering Cancer Center, New York, New York
Received 01/09/2008; revised 02/17/2008; accepted 02/22/2008.

Grant support: Resources from the HRH Prince Alwaleed Bin Talal Bin Abdulaziz Alsaud Institute for Computational Biomedicine, NIH grant T32 CA09685, and the Center for Cancer Prevention Research.

Note: Supplementary data for this article are available at Cancer Prevention Research Online (<http://cancerprevres.aacrjournals.org/>).

Requests for reprints: Harel Weinstein, Department of Physiology and Biophysics, Weill Medical College of Cornell University, Box 75, Room E-509, 1300 York Avenue, New York, NY 10065. Phone: 212-746-6358; Fax: 212-746-8690; E-mail: haw2002@med.cornell.edu.

©2008 American Association for Cancer Research.
doi:10.1158/1940-6207.CAPR-08-0007

mapping of interactions among differentially expressed genes based on information from interaction databases. Several different databases and tools were employed in this analysis of the observed global transcriptome changes in terms of biological functions and pathways, with the results suggesting that pathways related to cell proliferation, inflammation, apoptosis, and tissue injury were affected by TS. Finally, network representations of these data led to identification of proteins in the differentially expressed cohort that have multiple interaction partners (interaction hubs) and of transcription factors affected by TS. The analyses identified an epidermal growth factor receptor (EGFR)-centered network composed of several ligands of the EGFR that were induced by TS. Notably, aryl hydrocarbon receptor (AhR)-dependent genes induced by TS included the enzymes CYP1A1 and CYP1B1, which are of special interest because each may contribute to both carcinogenesis of the aerodigestive tract and drug metabolism (12–14). Consequently, we extended our analysis of TS-related transcriptome changes to human volunteers. Consistent with the *in vitro* findings presented here, we found increased levels of both CYP1A1 and CYP1B1 in the oral mucosa of healthy human subjects who smoked cigarettes. Further comparison of our findings in the MSK-Leuk1 cell model to *in vivo* data on transcriptome differences in airway epithelial cells of smokers (versus never smokers; ref. 15) identified a canonical set of differentially expressed genes and perturbed pathways. In addition to providing new insights into the procarcinogenic effects of TS, these findings highlight the potential of TS to alter the efficacy of pharmaceutical agents by inducing the expression of xenobiotic metabolizing enzymes.

Materials and Methods

Materials

Keratinocyte basal and growth media were supplied by Clonetics Corp. MuLV reverse transcriptase, oligo(dT)16, and RNase inhibitor were from Roche Applied Science, and Taq polymerase was from Applied Biosystems. HGU133 Plus 2 microarrays were from Affymetrix.

Tissue culture

The MSK-Leuk1 cell line was established from a dysplastic leukoplakia lesion adjacent to a squamous cell carcinoma of the tongue (16). Cells were routinely maintained in keratinocyte growth medium supplemented with bovine pituitary extract. Cells were grown in basal medium for 24 h before treatment. Treatment with vehicle (PBS) or TS was carried out on cells grown in growth factor-free basal medium. Cellular cytotoxicity was assessed by measurements of cell number, trypan blue exclusion, and release of lactate dehydrogenase. There was no evidence of cytotoxicity in our experiments.

Preparation of TS condensate

Cigarettes (2R4F, Kentucky Tobacco Research Institute) were smoked in a Borgwaldt piston-controlled apparatus (model RG-1) using the Federal Trade Commission standard protocol (17). The protocol variables attempt to mimic a standardized human smoking pattern (duration, 2 s/puff; frequency, 1 puff/min; volume, 35 mL/puff). Cigarettes were smoked one at a time in the apparatus and the smoke drawn under sterile conditions into premeasured amounts of sterile PBS (pH 7.4). This smoke in PBS represents whole trapped mainstream smoke abbreviated as TS. Quantitation of smoke content is expressed in puffs per milliliter, with one cigarette yielding ~8 puffs drawn into a 5-mL volume. The final TS concentration in cell culture medium is expressed as puffs per milliliter of medium.

Human tissue

Buccal mucosa specimens were obtained from nine never smokers and nine active smokers with a history of at least 10 pack-years. Subjects were excluded if they had gross evidence of oral inflammation, had a history of heavy alcohol consumption, or recently used nonsteroidal anti-inflammatory drugs or other anti-inflammatory medications. After topical anesthesia, 5-mm punch biopsies were obtained from grossly normal-appearing buccal mucosa. Tissue samples were immediately snap frozen in liquid nitrogen and stored at -80°C until analysis. H&E staining of representative formalin-fixed samples indicated that the biopsies were primarily composed of epithelium. This study was approved by the Committee on Human Rights in Research at Weill Cornell Medical College.

Reverse transcription-PCR

Total cellular RNA was isolated from cells using the RNeasy Mini Kit (Qiagen) according to the manufacturer's instructions. Reverse transcription was done with 2 μg of RNA per 50 μL of reaction. The reaction mixture contained 1 \times PCR buffer II, 2.5 mmol/L MgCl_2 , 0.5 mmol/L deoxynucleotide triphosphates, 2.5 $\mu\text{mol/L}$ oligo(dT)16 primer, 50 units of RNase inhibitor, and 125 units of MuLV. Samples were amplified in a thermocycler at 25°C for 10 min, 42°C for 15 min, 99°C for 5 min, and 5°C for 5 min. The resulting cDNA was then used for amplification. The volume of the PCR reaction was 25 μL and contained 5 μL of cDNA, 1 \times PCR buffer II, 2 mmol/L MgCl_2 , 0.4 mmol/L deoxynucleotide triphosphates, 400 nmol/L forward primer, 400 nmol/L reverse primer, and 2.5 units of Taq polymerase. Samples were denatured at 95°C for 2 min and then amplified for 30 cycles in a thermocycler under the following conditions: 95°C for 30 s, 62°C for 30 s, and 70°C for 45 s. Subsequently, the extension was carried out at 70°C for 10 min. Primers were synthesized by Sigma Genosys, and the sequences are listed in Supplementary Table S1.

To determine the levels of mRNAs for CYP1A1 and CYP1B1 in buccal mucosa, total RNA was isolated from biopsy samples with the RNeasy Mini Kit. Analysis was carried out as described above. Thermal cycling conditions were 95°C for 2 min, followed by 30 s at 95°C , 30 s at 62°C , and 45 s at 72°C for 30 cycles and then 72°C for 10 min. PCR products were subjected to electrophoresis on a 1% agarose gel with 0.5 $\mu\text{g/mL}$ ethidium bromide. The identity of each PCR product was confirmed by DNA sequencing. A computer densitometer (ChemDoc, Bio-Rad) was used to quantify the density of the different bands.

Microarray procedures

Biotinylated cRNAs were prepared according to the standard Affymetrix⁶ protocol from 2.5 μg of total RNA. Following fragmentation, 10 μg of cRNA were hybridized for 16 h at 45°C on GeneChip HG U133 Plus 2 arrays. GeneChips were washed and stained in Affymetrix Fluidics Station 450 and scanned with Affymetrix GeneChip Scanner 3000. At each of the five time points, six biological replicates were used for each TS treatment and another six biological replicates for vehicle-treated samples. In total, 60 chips were used.

Microarray data analysis

The gene annotations used for each probe set were from the February 2008 NetAffx HGU133 Plus 2 Annotation Files.

Preprocessing. Raw image data were background corrected, normalized, and summarized into probe set expression values using the Robust Multichip Average (RMA) algorithm. In our analysis, the largest variation in results arose from the method of preprocessing. Both the development of preprocessing methods and the assessment of results are active research areas and the choice of method affects the analysis outcome (18). RMA (19) and a modification, GC-RMA (20), have been shown to perform as well as, or better than, alternatives

⁶ <http://www.affymetrix.com>

using Plasmide data sets. However, GC-RMA can be biased when outliers are not eliminated. Further, both GC-RMA and another commonly used method, Affymetrix Microarray Analysis Suite v5.0 (MAS5), may perform poorly with highly variable human data (21). To check for the robustness of our results to different preprocessing methods, raw image data were preprocessed using both the RMA algorithm (19, 22) within GeneSpring 7.2 Software (Agilent Technologies) and MAS5, and then analyzed statistically as described below. We found a 75% agreement between RMA-preprocessed results and those from MAS5 (data not shown). This indicates a high level of consistency, as the overlap between RMA and MAS cited in the literature ranges from 27% (23) to 70% (18). In light of evaluation of the currently applicable methods in recent reviews (24), we performed both the statistical and functional inference analyses from the RMA-preprocessed data.

Normalization and filtering. The data from each chip were normalized for interarray comparisons as follows: measurements of <0.01 were set to 0.01 and each chip was normalized to 50% of the measurements taken from that chip (a procedure considered appropriate for large arrays when most of the genes are unaffected by experimental parameters). We further applied a filter to remove probe sets that were not reliably detected. From the complete set of ~54,675 probe sets on the HGU133 Plus 2 array, for every time point, we filtered out probe sets whose minimum raw expression level was not 50 in at least 2 of 12 conditions. This cutoff was chosen from the scatter plot distribution of expression values for TS versus vehicle-treated controls (marked as C). We further filtered out probe sets with low confidence if their *t*-test *P* value was not <0.05 in at least 2 of 12 conditions, using the Benjamini and Hochberg false discovery rate (FDR) criterion (25). Genes that passed these tests were defined as expressed and were statistically analyzed. This set of analyzed genes consists of the following numbers of probe sets: 20,791 (at 0.5 h), 20,443 (3 h), 20,979 (6 h), 19,584 (12 h), and 20,034 (24 h).

Statistical analysis. Probe sets were analyzed using both ANOVA and Significance Analysis of Microarrays (SAM). Genes that passed both SAM and ANOVA tests and had normalized expression values altered by a factor of 1.5-fold were deemed significant. ANOVA analysis was done using GeneSpring 7.2 software. SAM analysis was done using SAM Microsoft Excel plug-in. The details of this analysis are as follows: A one-way ANOVA was done at every time point using parametric test, not assuming variances equal (Welch's *t* test) with *P* < 0.05. To address the problem of multiple comparisons, Benjamini and Hochberg multiple testing correction was used to maintain FDR at 5% (25). The SAM method uses a set of gene-specific *t* tests, where each gene is assigned a score on the basis of its change in gene expression, relative to the SD of repeated measurements for that gene (26). Genes with scores greater than threshold δ values at FDR ~4% to 5% were deemed significant (because the FDR is dependent on δ value, an exact 5% FDR is not possible using the delta-slider within the SAM Excel plug in). At this δ value, the fold change parameter was set to 1.5. For input to SAM, two-class unpaired response was chosen on normalized data with *t*-statistics, 200 permutations, and default SAM options.

In summary, the analysis steps described above in comparing TS versus control at every time point are as follows: preprocessing (RMA) → normalization → filtering for expression → statistical analysis (SAM and ANOVA with multiple testing correction) → filtering for fold change.

Comparative analysis

Raw data (Affymetrix HGU133A chips) were downloaded from GEO repository.⁷ Smoking status-related genes in airway epithelia that are significantly differentially expressed were assessed using GeneSpring 7.2 as described above and separated into up-regulated

and down-regulated gene sets comprising 110 and 21 genes, respectively. Gene Set Enrichment Analysis (27) was used to compare the MSK-Leuk1 and airway epithelia gene expression results. The up-regulated and down-regulated gene sets in airway data were used to identify enrichment in the MSK-Leuk1 data. The MSK-Leuk1 expression data inputs were the normalized ratio values of all probe sets in HGU133 Plus 2 arrays and their collapsed HUGO symbols. Gene set enrichment analysis was done for every time point using default parameters, except the permutation type, which was gene set instead of phenotype (as recommended by the Gene Set Enrichment Analysis manual when number of replicates are <7). A reverse analysis was also done by using all the probe sets in airway epithelial data set as input and searching for enrichment on the significantly up-regulated or down-regulated gene sets at every time point of MSK-Leuk1 cell exposure to TS. Here, the differentially expressed gene sets in MSK-Leuk1 data were collapsed to the HUGO symbols of probe sets available in HGU133A microarrays.

Leading-edge subset. The leading-edge subset is defined as comprising those members of the gene set that appear in the ranked list at, or before, the point where the running sum reaches its maximum deviation from zero. The set is suggested to be the core of a gene set that accounts for the enrichment score (27).

Functional analysis

To relate the results to cell physiologic mechanisms, the transcriptional data were integrated with available experimental signaling data for TS. The complex biological processes induced by TS were examined in the context of detailed protein-protein interaction maps (28) and molecular networks (29). The interaction networks shown in Figs. 1C and 2A were generated with Ingenuity Pathways Analysis (IPA), a web-delivered application used to discover, visualize, and explore relevant networks (29). Affymetrix probe identifiers were uploaded to IPA, each identifier was mapped to its corresponding gene object in the Ingenuity Pathways Knowledgebase, and only direct interactions were considered. For the network in Fig. 2A, interactions were queried between these gene objects and all other gene objects stored within IPA to generate a set of networks that were then merged. The only putative hubs considered in the merged network were transcription regulators that are expressed in MSK-Leuk1 cells and have at least six direct interactions with differentially expressed genes.

For functional categories, Ingenuity Knowledgebase (29) and Gene Ontology (GO)⁸ databases were searched for categories statistically enriched in the differentially expressed genes set, and the likelihood of perturbations in each category was scored. In searching GO categories, the EASE software (30) was used to compare the Affymetrix probe identifiers of differentially expressed genes with the list of all probes in the HGU133 Plus 2 microarray.

We reasoned that a small but coherent difference in the expression of a group of genes in a category or pathway can be more important than large differences in unrelated genes. Therefore, we carried out categorization and pathway-enrichment analyses that enabled identification and scoring of both significant and modest perturbations in corresponding gene groups. For a functional analysis that can capture modest perturbations in functional groups, we used all expressed genes (as defined above in "Microarray data analysis"). Hence, we identified groups of genes that correspond to specific enzymatic, metabolic, or signaling pathways within pathway databases of KEGG⁹ and BioCarta¹⁰ using the PLAG tool (31) and the SAFE tool (32) within GO categories. Note that we did not use a FDR or family-wise error rate estimate for functional groups. Whereas this might result in an increase in type II estimates, it is acceptable because we focused

⁷ <http://www.ncbi.nlm.nih.gov/geo/>

⁸ <http://www.geneontology.org>

⁹ <http://www.genome.jp/kegg>

¹⁰ <http://biocarta.com/genes/index.asp>

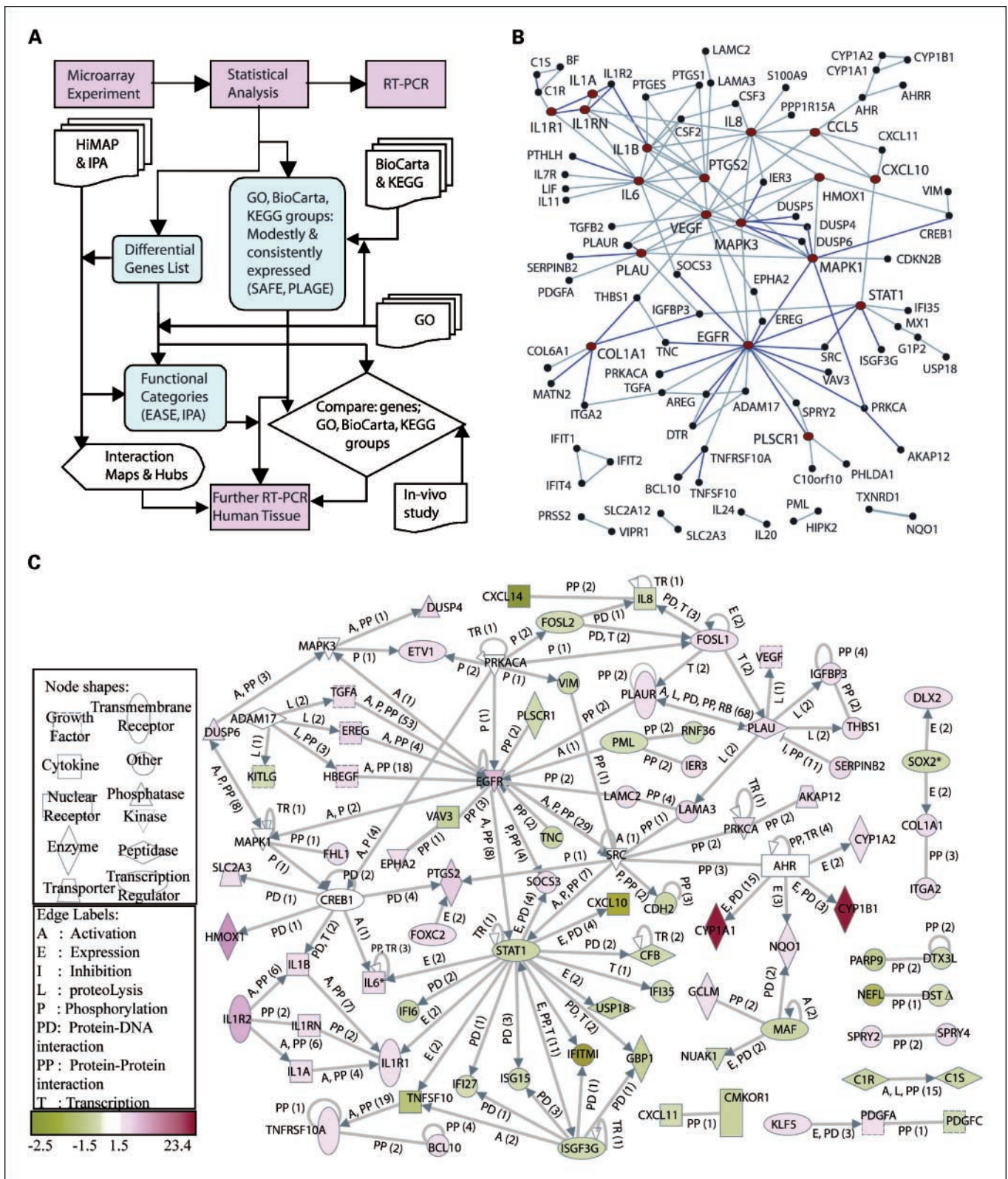


Fig. 1. A, flowsheet describing the systematic analysis of TS-induced changes in the transcriptome of MSK-Leuk1 cells, including hypothesis generation steps. B, protein-protein interaction network of differentially expressed genes (<http://www.physiology.med.cornell.edu/go/smoke>) and signaling proteins known to be activated by TS [Ahr, ADAM17, CREB1, MAPK3 (ERK1), MAPK1 (ERK2), PRKACA, and SRC] within HIMAP database, which includes interactions that are literature confirmed from the Human Protein Reference Database (ref. 40; blue), yeast two-hybrid defined (gray), or predicted based on function (gray). Hubs with four or more connections (red) are CCL5, COL1A1, CXCL10, EGFR, HMOX1, IL1A, IL1B, IL1RN, IL1R1, IL6, IL8, MAPK1, MAPK3, PTGS2, PLAUR, PLSCR1, STAT1, and VEGF. C, direct interaction network of differentially expressed genes and known TS-activated signaling proteins generated using IPA (29). At each edge, the interaction type is shown and the number of publications is indicated in parentheses. Hubs are listed in Supplementary Table S2.

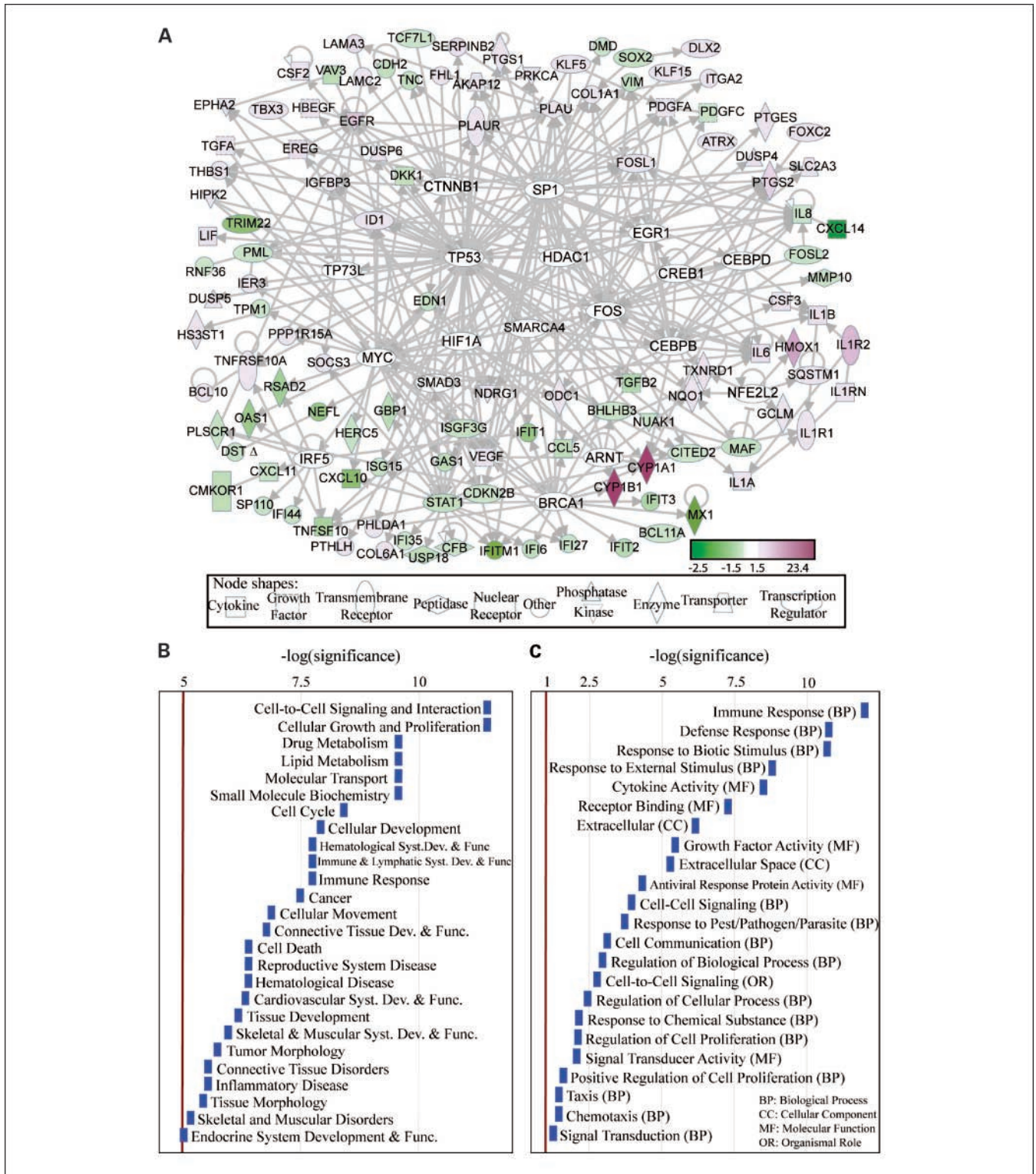


Fig. 2. A, direct interaction network of differentially expressed genes in TS-treated MSK-Leuk1 cells, integrated with genes related to signaling proteins known to be activated by TS. The white nodes are genes with no significant expression change due to TS in our analysis, but which are expressed in MSK-Leuk1 cells (filtered as in Materials and Methods, statistical analysis) and interact with at least six differentially expressed genes, suggesting potential roles for these in TS-perturbed signaling processes. These include *ARNT*, *BRCA1*, *CEBPB*, *CEBPD*, *CREB1*, *CTNNB1*, *EGR1*, *FOS*, *HDAC1*, *HIF1A*, *IRF5*, *MYC*, *NFE2L2*, *SMAD3*, *SMARCA4*, *SP1*, *TP53*, and *TP73L*. IPA tool (29) was used to generate the merged networks. B, statistically significant diseases and physiologic, cellular, or molecular functions of the differentially expressed genes. The bars are sized according to the calculated $-\log(\text{significance})$ score. C, statistically overrepresented groups in GO Biological Process (BP), GO Molecular Function (MF), GO Cellular Components (CC), and organismal role among the differentially expressed genes as compared with the set of genes in the microarray, generated with EASE software, based on overrepresented chromosomes, organismal roles, GO categories, and pathway categories within KEGG, GenMAPP (<http://www.genmapp.org>), and BBID (<http://bbid.grc.nia.nih.gov>) databases. Categories with Bonferroni $P < 0.05$ were assumed significant, and Affymetrix identifiers were used.

Table 1. Time-dependent effects of TS on gene expression in MSK-Leuk1 cells

Gene name	Affymetrix ID	0.5 h		3 h		6 h		12 h		24 h		Description
		Fold	P	Fold	P	Fold	P	Fold	P	Fold	P	
<i>CYP1A1</i>	205749_at	13.4	3.3e-06	17.4	2.1e-08	23.4	1.1e-07	11.3	1.5e-06	14.3	1.0e-05	Cytochrome P450, family 1, subfamily A, polypeptide 1
<i>CYP1B1</i>	202437_s_at	8.3	4.2e-06	14.1	4.0e-06	13.5	1.7e-06	5.8	5.5e-06	6.1	2.1e-08	Cytochrome P450, family 1, subfamily B, polypeptide 1
<i>CYP1B1</i>	202435_s_at	8.1	3.8e-06	11.4	1.2e-06	12.1	1.7e-06	6.7	4.3e-05	6.1	1.2e-04	Cytochrome P450, family 1, subfamily B, polypeptide 1
<i>CYP1B1</i>	202436_s_at	7.4	4.3e-06	11.0	4.5e-05	11.2	5.5e-08	6.0	1.5e-06	5.9	1.7e-04	Cytochrome P450, family 1, subfamily B, polypeptide 1
<i>IL24</i>	206569_at	2.8	5.8e-04	3.4	4.0e-06	2.8	3.6e-04	3.7	7.9e-04	2.8	1.7e-03	Interleukin-24
<i>PTGS2</i>	1554997_a_at	2.7	7.0e-03	3.0	1.0e-03	3.0	4.0e-03	3.1	2.3e-03	3.0	4.8e-04	Prostaglandin-endoperoxide synthase 2 (COX-2)
<i>EREG</i>	205767_at	2.1	1.8e-03	2.6	4.0e-06	2.2	3.8e-05	2.4	8.2e-05	2.0	1.0e-04	Epiregulin
<i>LOC151438</i>	1560679_at	2.1	8.7e-03	1.9	1.4e-02	1.5	3.7e-02	3.2	2.1e-02	5.9	6.8e-05	Hypothetical protein LOC151438
<i>PTGS2</i>	204748_at	2.1	1.2e-04	2.7	1.6e-04	2.4	2.6e-03	3.2	6.1e-04	2.9	1.5e-04	Prostaglandin-endoperoxide synthase 2 (COX-2)
<i>TIPARP</i>	212665_at	2.0	2.2e-06	3.0	9.3e-09	2.2	1.7e-06	2.2	1.5e-06	2.0	1.0e-04	TCDD-inducible poly(ADP-ribose) polymerase
<i>IL1B</i>	205067_at	1.9	1.3e-04	2.2	3.5e-07	2.1	3.1e-06	2.1	5.5e-06	2.1	6.4e-05	Interleukin-1β
<i>ALDH1A3</i>	203180_at	1.9	1.9e-04	2.0	9.8e-09	2.4	2.8e-06	2.0	1.3e-03	2.8	2.8e-04	Aldehyde dehydrogenase 1 family, member A3
<i>IL1R2</i>	211372_s_at	1.9	8.4e-06	1.7	1.9e-02	1.9	5.6e-04	2.9	2.2e-03	5.0	4.6e-04	Interleukin-1 receptor, type II
<i>IL1R2</i>	205403_at	1.8	1.1e-05	1.6	1.6e-02	1.8	5.2e-03	2.7	3.8e-03	5.3	6.6e-04	Interleukin-1 receptor, type II
<i>IL1B</i>	39402_at	1.8	2.9e-05	2.1	2.1e-08	2.0	1.7e-06	1.9	5.5e-06	2.2	9.4e-05	Interleukin-1β
<i>IL20</i>	224071_at	1.7	8.3e-03	2.1	6.4e-05	1.8	4.6e-04	1.7	1.5e-02	1.7	2.7e-03	Interleukin-20
<i>DUSP4</i>	204014_at	1.7	1.3e-02	1.6	2.5e-03	1.7	1.2e-04	2.3	2.3e-04	2.4	5.4e-04	dual specificity phosphatase 4
	226034_at	1.6	8.6e-03	1.6	2.6e-04	1.5	3.4e-04	2.1	2.4e-03	2.0	4.4e-04	Clone IMAGE:3881549, mRNA
<i>SERPINB2</i>	204614_at	1.6	2.9e-03	1.6	5.8e-04	1.6	2.4e-04	1.9	1.8e-04	2.5	1.0e-05	Serine (or cysteine) proteinase inhibitor, clade B (ovalbumin), member 2
<i>LOC344887</i>	241418_at	1.5	5.0e-02	3.6	2.9e-05	4.2	5.5e-08	2.6	8.8e-05	1.9	9.8e-04	Similar to NmrA-like family domain containing 1
<i>MAF</i>	209348_s_at	-1.5	1.9e-04	-1.5	2.7e-02	-1.5	1.8e-02	-1.7	2.1e-02	-1.8	1.7e-03	v-maf musculoaponeurotic fibrosarcoma oncogene homologue (avian)
<i>PRICKLE1</i>	226069_at	-1.6	4.1e-02	-1.6	1.2e-02	-2.2	2.0e-03	-1.6	2.8e-02	-2.0	7.7e-04	Prickle homologue 1 (<i>Drosophila</i>)
<i>NAV2</i>	218330_s_at	-1.7	3.8e-03	-1.8	1.3e-02	-1.7	2.0e-03	-1.7	3.7e-03	-1.8	1.0e-04	Neuron navigator 2
<i>FILIP1L</i>	204135_at	-1.7	3.8e-06	-2.1	7.1e-06	-2.2	1.3e-05	-2.4	1.9e-03	-2.1	6.4e-05	Filamin A interacting protein 1-like
<i>FILIP1L</i>	1554966_a_at	-1.7	8.4e-06	-2.2	6.4e-05	-2.2	2.0e-06	-2.5	1.5e-03	-2.2	1.0e-04	Filamin A interacting protein 1-like
<i>C10orf10</i>	209183_s_at	-2.0	6.1e-04	-2.3	1.2e-03	-2.1	4.4e-05	-2.3	4.3e-05	-2.1	6.4e-05	Chromosome 10 open reading frame 10
<i>TNFSF10</i>	202688_at	-2.0	8.7e-03	-1.7	1.3e-02	-2.4	4.2e-03	-2.3	4.8e-04	-2.4	1.9e-04	Tumor necrosis factor (ligand) superfamily, member 10

NOTE: Fold-differences and *P* values are shown at each time point. Detailed lists and annotations are provided at <http://physiology.med.cornell.edu/go/smoke>.

particularly on pathways that seem to be consistently perturbed at multiple time points.

Clustering

An unsupervised hierarchical clustering analysis across all samples of the microarray data was done for the probe sets found to be differentially expressed between control and TS-treated cells at any of the five time points (using log-transformed normalized data). A Pearson correlation (uncentered) similarity metric and average linkage clustering was done with Cluster and TreeView software¹¹ (see Supplementary Fig. S1). Our study was not designed to identify the dynamic effects of TS so that limitation to five time points results in a rather sparse matrix for such analysis under the commonly used tools [CAGED (33) and SSCLUST (34)]. Further results from the use of a newly described clustering algorithm, EP_GOS_Clust (35), were used to classify the time-dependent patterns of changes in gene expression and will be reported as a separate study.

Additional information

The complete list of differentially expressed genes and functional groups at every time point is made available through an interactive web site¹² established as a resource of the Institute for Computational Biomedicine. Also available at that site are the results from the functional analyses of the *in vivo* data for comparative purposes. The microarray data have been deposited at the National Center for Biotechnology Information Gene Expression Omnibus (GEO)¹³ under GEO Series accession no. GSE10063.

Results

The effect of TS on gene expression was determined in MSK-Leuk1 cells. Based on microarray analysis, exposure to TS led to at least a 1.5-fold change in the expression of 411 probe sets. The complete list of genes and the expression levels measured under the experimental conditions described here are available online.¹⁴ The number of differentially expressed genes was observed to increase with duration of exposure to TS, amounting to 91, 104, 106, 166, and 274 probe sets at 0.5, 3, 6, 12, and 24 hours, respectively. The heatmap representation of the results from the clustering of the differentially expressed genes (see Materials and Methods) is shown in Supplementary Fig. S1. The results show that replicate samples at each time point cluster together and that TS-treated samples and controls are separated into distinct clusters. Twenty-seven probe sets corresponding to 20 unique genes were differentially expressed at every time point signifying a persistent change in expression (Table 1). Subsequently, reverse transcription-PCR was used to validate microarray findings for a subset of 10 differentially expressed genes. The observed changes in expression were quantitatively consistent with the microarray results in showing that exposure to TS led to increased levels of mRNAs for CYP1A1, CYP1B1, PTHLH, IL1B, EREG, ALDH1A3, IL6, and IL24, and to reduced expression of TNFSF10 and CCL5 (data not shown). Thus, the reverse transcription-PCR results were entirely consistent with the microarray predictions for all 10 genes evaluated, validating the experiment and statistical analyses. Furthermore, our findings are consistent with published studies in which treatment of MSK-Leuk1

cells with TS induced the following genes: cyclooxygenase COX-2 (*PTGS2*; ref. 17), amphiregulin (*AREG*; refs. 17, 36), and transforming growth factor α (*TGFA*; ref. 17).

Interpreting the global transcriptome changes in terms of biological functions and pathways

Several databases and tools were used to classify the differentially expressed genes into relevant molecular, physiologic, and disease categories. TS-induced transcriptome changes were related to cellular processes and pathways using molecular network maps, hubs, functional classes, and enrichment analysis. Details of this rigorous functional analysis are represented in a flowsheet format in Fig. 1A.

Network analysis. The differentially expressed gene set was integrated with the set of signaling proteins previously shown to be activated by TS: ADAM17 (37), AhR (36, 38), cyclic AMP responsive element binding protein 1 (CREB1; ref. 36), mitogen-activated protein kinase [extracellular signal-regulated kinase (ERK)-1/2; ref. 39], protein kinase A catalytic subunit (PRKACA; ref. 36), and SRC.¹⁵ Assuming that highly interconnected networks likely represent significant biological function, we sought to identify the interrelations among these genes.

Protein-protein interactions. Direct physical relationships between proteins associated with the gene set were identified using the human protein-protein interaction map HiMAP (28), as shown in Fig. 1B. The proteins found to have four or more possible physical interactions are listed in Supplementary Table S2. Hubs with the most Human Protein Reference Database (40) connections (blue edges in Fig. 1B) are *MAPK3*, *COL1A1*, and *EGFR*. In fact, an EGFR-centered subnetwork was observed, where EGFR and its ligands EREG, AREG, DTR (HB-EGF), and TGFA are all significantly induced.

Interactions based on mammalian biology data. The interactions within the set of TS-modified genes were mapped in the context of the network of physical, transcriptional, and enzymatic interactions observed in mammals. The results (obtained using the Ingenuity Pathway Analysis Tool, IPA; ref. 29) are represented in Fig. 1C. The interactions considered were proteolysis, inhibition, protein-protein interaction, expression, protein-DNA interaction, activation, and transcription (29). Among hub proteins (listed in Supplementary Table S2), EGFR, PLAU, IL1R1, and related proteins are mainly induced (shown in red), whereas STAT1 and related proteins are repressed (shown in green). Interestingly, cytokines form a subnetwork composed of IL1R1, IL1R2, IL1A, IL1B, and IL1RN, suggesting a TS-induced inflammatory process. Another hub, formed around PLAU, involves genes that contribute to invasiveness (39). At the stringency level used for the initial analysis of TS-affected gene expression, AhR expression was not considered significantly altered, but the likely role of the AhR is evident from the effect of TS on genes known to be regulated by this receptor. Specific examples include the observed increased levels of CYP1A1, CYP1B1, and AREG, which are known targets of ligand-activated AhR (36, 38). In a similar manner, various transcription regulators connected to large numbers of differentially expressed genes

¹¹ Cluster and TreeView were obtained at <http://rana.lbl.gov/EisenSoftware.htm>.

¹² <http://physiology.med.cornell.edu/go/smoke>

¹³ <http://www.ncbi.nlm.nih.gov/geo/>

¹⁴ <http://physiology.med.cornell.edu/go/smoke>

¹⁵ Unpublished data.

can have important roles in signaling pathways perturbed by TS. Mapping the direct interaction network of differentially expressed genes and transcription regulators can reveal such involvement. Shown in Fig. 2A are highly connected putative transcription regulators in response to TS, including sp1 transcription factor (SP1), catenin β 1 (CTNNB1), IFN regulatory factor 5 (IRF5), histone deacetylase 1 (HDAC1), tumor protein p53 (TP53), tumor protein p73-like (TP73L), hypoxia inducible factor 1, α subunit (HIF1A), nuclear factor (erythroid-derived 2)-like 2 (NFE2L2), cellular oncogene c-fos (FOS), myc proto-oncogene protein (MYC), early growth response (EGR1), and a number of well-studied transcription factors and cancer-related genes that included BRCA1, CEBPB, CEBPD, and the AhR nuclear translocator (ARNT). We note that the AhR and hypoxia signaling pathways have been shown to cross-talk via the involvement of HIF1 α (41), and whereas HIF1 α does not seem to be significantly altered, our analysis suggests its involvement in signaling pathways as a transcription regulator hub.

Gene classification. Classification of statistically significant genes into biological categories. The genes affected by

TS were also classified into related diseases and molecular, cellular, and physiologic functions based on the information from the largest literature curated information database, IPA (Fig. 2B; ref. 29). Cancer is the most relevant disease and the most relevant functions are cell-to-cell signaling and interaction, cellular growth and proliferation, drug and lipid metabolism, immune response, and connective tissue development and function. We further categorized genes in terms of relevant functional categories using public databases of controlled vocabulary including GO (Fig. 2C; Supplementary Table S3). The information from these databases also confirms that genes related to cell proliferation and immune responses are overrepresented. As the examples above suggest, the classification of differentially expressed genes is inherently sensitive to the statistical analysis results and filtering criteria. We therefore identified an additional category of statistically significant modestly perturbed functional groups of genes among all expressed genes in the MSK-Leuk1 cells and defined their functional categories using the GO, KEGG, and BioCarta databases. Pathways consistently perturbed at multiple time points are given in Table 2.

Table 2. Treatment of MSK-Leuk1 cells with TS affected pathways related to cell proliferation, inflammation, apoptosis, coagulation, and tumor suppression

	0.5 h	3 h	6 h	12 h	24 h
	<i>P</i> (genes/path)				
KEGG pathways					
Cytokine-cytokine receptor interaction	↑0.0025(84/257)	↑<1e-4(86/257)	↑9e-04(83/257)	↑0.0008(79/257)	↑0.0025(83/257)
Prostaglandin and leukotriene metabolism	↑0.0447(15/39)	↓0.007(15/39)	↑0.044(15/39)	↑0.008(15/39)	↑0.0025(15/39)
Neuroactive ligand-receptor interaction	↑0.0025(43/295)	↓0.032(46/295)	↓0.02(51/295)	↑0.0025(39/295)	↑<1e-4(46/295)
γ -Hexachlorocyclohexane degradation	↑0.0092(13/45)	↑0.003(13/45)	↑0.008(13/45)	↑0.0025(11/45)	↑0.0041(14/45)
Hedgehog signaling pathway	↑0.0117(21/53)	↑0.003(21/53)	↓0.009(23/53)	↑0.0025(20/53)	↓0.0025(22/53)
Complement and coagulation cascades	↑0.0025(20/69)	↑0.003(21/69)	↑0.008(21/69)	↑0.0025(18/69)	↑0.0025(19/69)
Porphyrin and chlorophyll metabolism		↓0.003(16/32)	↑0.011(16/32)	↑0.0132(16/32)	↑0.0203(16/32)
Amino sugar metabolism	↑0.0025(24/27)	↓0.007(24/27)		↑0.0349(24/27)	↑0.0218(24/27)
Jak-STAT signaling pathway	↑0.0025(81/159)	↑0.012(81/159)		↑0.0025(78/159)	↑0.0025(81/159)
Biocarta pathways					
Msp/Ron receptor signaling pathway	↓0.0001(4/6)	↓0.0025(5/6)	↓0.0134(5/6)	↓0.01(5/6)	↓0.0025(5/6)
Cytokine network	↑0.0025(5/22)	↑0.0025(5/22)	↑0.0025(5/22)	↑0.003(5/22)	↑0.0025(5/22)
Regulation of hematopoiesis by cytokines	↑0.0025(6/15)	↑0.0025(6/15)	↑0.0418(6/15)	↑0.046(6/15)	↑0.0025(6/15)
Cytokines and inflammatory response	↑0.0025(11/29)	↑<1e-4(11/29)	↑0.0008(11/29)	↑0.003(11/29)	↑<1e-4(11/29)
Fibrinolysis pathway	↑0.0025(6/12)	↑0.0049(6/12)	↑0.0025(6/12)	↑0.003(5/12)	↑0.0044(6/12)
Mechanism of acetaminophen activity and toxicity	↑0.0025(3/6)	↑0.0025(3/6)	↑0.0025(3/6)	↑<1e-4(3/6)	↑0.0025(3/6)
Signal transduction through IL1R	↑0.0152(28/33)	↑0.0025(28/33)	↑0.0095(28/33)	↑0.003(28/33)	↑0.0044(28/33)
Erythrocyte differentiation pathway	↑0.0025(7/15)	↑0.0025(7/15)	↑0.0025(7/15)	↑0.013(7/15)	↑0.0044(7/15)
Mechanism of gene regulation by peroxisome proliferators via PPAR α	↑0.0025(43/57)		↑0.0197(42/57)	↑0.013(42/57)	↑0.0096(42/57)
Cells and molecules involved in local acute inflammatory response	↑0.0025(7/17)	↑0.0364(8/17)	↓0.0169(8/17)		↑0.0025(7/17)
IL-10 anti-inflammatory signaling pathway	↑0.0025(11/13)	↓0.0076(11/13)	↑0.0025(11/13)		↓0.0025(11/13)
Stress induction of HSP regulation	↑0.0025(12/15)		↑0.0025(12/15)	↑0.006(11/15)	↓0.0044(11/15)
Extrinsic prothrombin activation pathway		↑0.0393(5/13)	↑0.0291(4/13)	↑0.013(4/13)	↑0.0189(4/13)
p53 signaling pathway		↓0.0076(13/15)	↓0.0446(14/15)	↓0.013(13/15)	↓0.0025(13/15)

NOTE: *P* values are presented. Complete lists per time point are provided at <http://physiology.med.cornell.edu/go/smoke>. Generated using PLAGE tool (31).

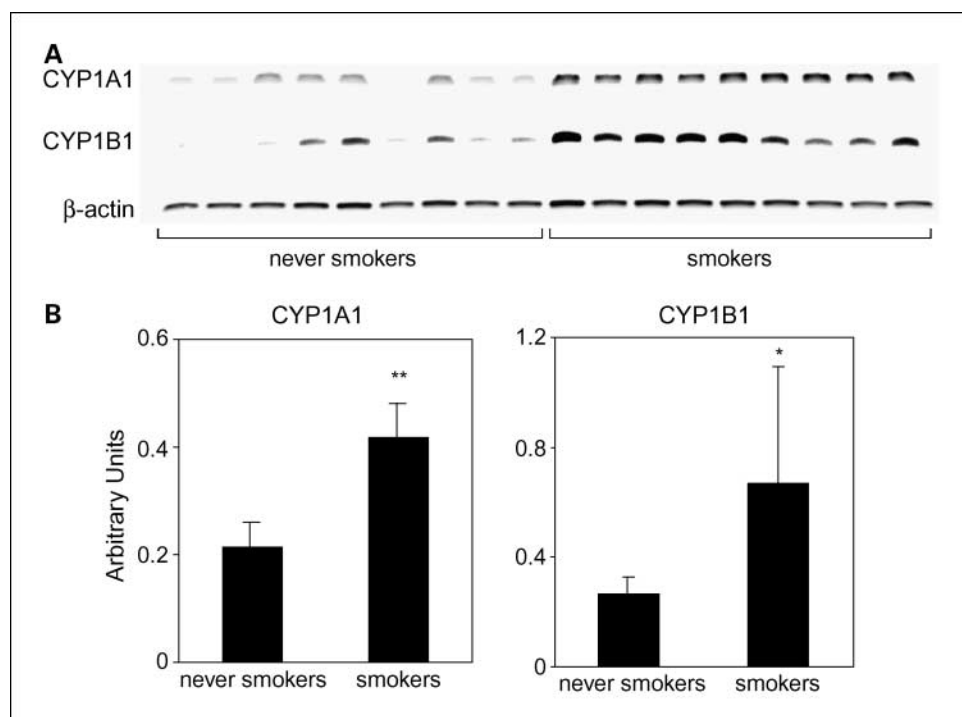


Fig. 3. Levels of CYP1A1 and CYP1B1 are increased in the oral mucosa of cigarette smokers. **A**, oral mucosal biopsies were obtained from both never smoking (*never smokers*; $n = 9$) and smoking (*smoker*; $n = 9$) human volunteers. Total cellular RNA was extracted from the oral mucosal biopsy samples and reverse transcribed. The expression of CYP1A1 and CYP1B1 mRNAs was assessed by reverse transcription-PCR. No bands were observed when cDNA was omitted from the PCR reaction or when the reverse transcriptase enzyme was not included in the reverse transcriptase reaction. **B**, results of the data shown in **A** expressed in arbitrary units. Columns, mean; bars, SD. *, $P < 0.05$; **, $P < 0.01$, versus never smokers.

Increased levels of CYP1A1 and CYP1B1 were detected in the oral mucosa of human cigarette smokers

Because the analysis suggested that CYP1A1 and CYP1B1 (AhR-dependent genes) were the two genes most induced by TS treatment of MSK-Leuk1 cells (Table 1), we next investigated whether the *in vitro* results were predictive of increased levels of CYP1A1 and CYP1B1 mRNAs in the oral mucosa of human smokers. To this end, we carried out a comparative analysis in the oral mucosa of healthy cigarette smokers versus never smoking human volunteers. Consistent with the findings in MSK-Leuk1 cells (Table 1), the amounts of CYP1A1 and CYP1B1 mRNAs were both increased in the oral mucosa of smokers (Fig. 3).

Comparison to airway epithelial transcriptome of smokers and nonsmokers

The acute effects of TS on the transcriptome of MSK-Leuk1 cells were compared with published chronic transcriptome differences measured in airway epithelial cells of 34 current smokers and 23 never smokers (15). To minimize preprocessing and statistical methodology-based differences, these human data were reanalyzed using the same statistical tools used here. The comparison revealed that the genes strongly overexpressed due to TS in MSK-Leuk1 cells, namely, CYP1A1, CYP1B1, ALDH1A3, GCLM, TXNRD1, NQO1, PIR, and AKR1C1, were also induced in the bronchial airways of smokers compared with nonsmokers, whereas MMP10 is repressed in both (Table 3). Pathways and functional categories consistently altered in both groups are given in Supplementary Tables S4 and S5.

We further explored the similarity between the gene expression data sets from airway epithelia and MSK-Leuk1 cells by comparing relative enrichment using the Gene Set Enrichment Analysis method (27) as described in Materials and Methods. At every time point, the TS-treated MSK-Leuk1 gene set was

found to be significantly enriched in genes up-regulated in airway epithelial cells (FDR < 0.001); a significant negative correlation was observed in this analysis with the down-regulated genes (FDR = 0.019, 0.001, 0.037, 0.004, and 0.01 for 0.5, 3, 6, 12, and 24 hours, respectively). In the reverse analysis, the airway data set was found to be significantly enriched in genes induced in MSK-Leuk1 cells at every time point (FDR = 0.043, 0.009, 0.011, 0.009, and 0.048 for 0.5, 3, 6, 12, and 24 hours, respectively). Thus, the results from this Gene Set Enrichment analysis identify significant correlations between the sets of data from the two experiments, and further support the use of the MSK-Leuk1 cell line as a model for detailed mechanistic studies on TS effects.

The *leading-edge subsets* of the significant gene sets in airway epithelia include 50 up-regulated and 16 down-regulated genes. Of these, ALDH1A3, CYP1A1, CYP1B1, GCLM, GPX2, NQO1, PIR, SERPINB13, SLC7A11, TXNRD1, and UGT1A10 /// UGT1A8 are members of a consistently induced subset (in at least four time points). At the same time, KAL1, MMP10, NFKB1A, and TMEM45A are members of a consistently repressed subset (in at least four time points) in both sets of experiments. The highest number of leading-edge subset genes in the airway epithelial data are for the 0.5-hour time point, which is interesting because this time point does not have the largest number of differentially expressed genes. The reverse analysis, for the leading-edge subsets of the significantly up-regulated genes in MSK-Leuk1 data, results in a total of 20 genes enriched in airway epithelial cells. The complete set of results is given in Supplementary Table S6. Details of this analysis and the related html files are available online.¹⁶

¹⁶ <http://physiology.med.cornell.edu/go/smoke>

Table 3. Genes that are differentially expressed in both the airways of human smokers and MSK-Leuk1 cells exposed to TS for 0.5 to 24 h with associated *P* values

Symbol	ID	Human airway	0.5 h	3 h	6 h	12 h	24 h	Description
			<i>P</i>					
<i>CYP1A1</i>	205749_at	↑4.4e-04	↑3.3e-06	↑2.1e-08	↑1.1e-07	↑1.5e-06	↑1.0e-05	Cytochrome <i>P</i> 450, family 1, subfamily A, polypeptide 1
<i>CYP1B1</i>	202436_s_at	↑1.7e-07	↑4.3e-06	↑4.5e-05	↑5.5e-08	↑1.5e-06	↑6.6e-04	Cytochrome <i>P</i> 450, family 1, subfamily B, polypeptide 1
<i>CYP1B1</i>	202437_s_at	↑8.5e-08	↑4.2e-06	↑4.0e-06	↑1.7e-06	↑5.5e-06	↑2.1e-08	Cytochrome <i>P</i> 450, family 1, subfamily B, polypeptide 1
<i>GCLM</i>	203925_at	↑1.8e-05	↑1.5e-03	↑1.3e-03	↑3.4e-04	↑1.8e-04	↑3.5e-03	Glutamate-cysteine ligase, modifier subunit
<i>TXNRD1</i>	201266_at	↑6.0e-07	↑1.2e-02	↑2.7e-04	↑4.9e-05	↑8.8e-05	↑1.6e-03	Thioredoxin reductase 1
<i>ALDH1A3</i>	203180_at	↑1.5e-04	↑1.9e-04	↑9.8e-09	↑2.8e-06	↑1.3e-03	↑2.8e-04	Aldehyde dehydrogenase 1 family, member A3
<i>NQO1</i>	201468_s_at	↑2.8e-13	↑4.7e-05	↑2.3e-05	↑1.3e-06	↑6.6e-04	↑1.8e-04	NAD(P)H dehydrogenase, quinone 1
<i>NQO1</i>	201467_s_at	↑4.7e-12	3.2e-02	>0.05	↑9.0e-05	↑4.0e-03	↑4.8e-03	NAD(P)H dehydrogenase, quinone 1
<i>PIR</i>	207469_s_at	↑1.3e-12	>0.05	>0.05	↑2.8e-02	↑3.1e-02	↑3.2e-02	Pirin
<i>AKR1C1</i>	204151_x_at	↑1.4e-10	↓2.8e-02	>0.05	↑3.8e-03	↑1.5e-02	↑6.0e-04	Aldo-keto reductase family 1, member C1
<i>NQO1</i>	210519_s_at	↑3.1e-14	↓4.7e-02	↑1.3e-02	↑2.0e-05	↑2.1e-03	↑3.7e-04	NAD(P)H dehydrogenase, quinone 1
<i>AKR1C1</i>	216594_x_at	↑1.2e-09	>0.05	>0.05	↑2.4e-04	↑8.1e-03	↑9.3e-03	Aldo-keto reductase family 1, member C1
<i>AKR1C2</i>	211653_x_at	↑4.0e-12	>0.05	>0.05	↑9.6e-03	↑2.3e-02	↑1.6e-04	Aldo-keto reductase family 1, member C2
<i>AKR1C2</i>	209699_x_at	↑2.5e-14	↑3.8e-02	>0.05	↑2.5e-03	>0.05	↑4.4e-04	Aldo-keto reductase family 1, member C2
<i>MMP10</i>	205680_at	↓5.6e-04	>0.05	>0.05	↓2.2e-02	>0.05	>0.05	Matrix metalloproteinase 10 (stromelysin 2)

Discussion

We characterized here the effects of TS on gene expression and cellular pathways in MSK-Leuk1 cells. As these were shown to relate to xenobiotic metabolism, cell proliferation, apoptosis, and cell movement, the results can potentially bring a new level of understanding to the complex biological effects of TS, and in particular to the manner cellular mechanisms are perturbed leading to carcinogenesis. Cancer patients who continue to smoke have a worse prognosis than individuals who quit smoking, but the underlying mechanisms are poorly understood. The specific pathways shown here to be affected, as well as the identified hubs in the networks composed of the differentially expressed genes, should provide insights into not only the putative mechanisms by which TS affects carcinogenesis but also the manner in which it might affect cancer treatment outcome. Of special note in this context is that TS induced *CYP1A1* and *CYP1B1* both *in vitro* and *in vivo*. More specifically, increased levels of *CYP1A1* and *CYP1B1* were found in MSK-Leuk1 cells exposed to TS and in the oral mucosa of humans who smoked cigarettes heavily, results that confirm and amplify a previous report of elevated levels of *CYP1B1* in exfoliated buccal mucosal cells from smokers (42). Because both *CYP1A1* and *CYP1B1* convert a broad array of carcinogens to active metabolites that can form DNA

adducts, it becomes important to consider the potential implications of TS-mediated induction of these enzymes. Thus, several classes of carcinogens (e.g., polycyclic aromatic hydrocarbons, nitroaromatics, and arylamines) are activated to mutagenic derivatives by these enzymes (43, 44). It is possible that TS-mediated induction of *CYP1A1* and *CYP1B1* will increase the mutagenic effects of these carcinogens. The potential significance of such an effect is underscored by the finding that B[a]P diol epoxide, a mutagen formed by *CYP1A1* or *CYP1B1*, causes adducts along the exons of the *TP53* gene that correspond to p53 hotspots in human tumors (45). Based on these results, one potential chemopreventive strategy would be to identify agents that suppress the TS-mediated induction of *CYP1A1* and *CYP1B1*.

In addition to being able to activate carcinogens, *CYP1A1* and *CYP1B1* play a role in the metabolism of several anticancer drugs including docetaxel, tamoxifen, and erlotinib (6, 46). Recently, erlotinib, a small-molecule inhibitor of EGFR tyrosine kinase, was found to be more effective in the treatment of patients with non-small cell lung cancer who were never smokers compared with smokers (10). Reduced levels of erlotinib were found in the plasma of smokers compared with never smokers, suggesting increased metabolic clearance (6). Our finding that *CYP1A1* and *CYP1B1* levels are increased

in the oral mucosa of smokers raises the distinct possibility that, in addition to systemic clearance, local clearance of erlotinib will be enhanced in smokers, leading to decreased clinical benefit. Collectively, these findings underscore the need for both a more careful monitoring of smoking status in clinical trials and increased smoking cessation efforts in cancer patients. Studies are under way or being planned to evaluate the efficacy of erlotinib in the prevention and treatment of head and neck squamous cell carcinoma.

The induction of CYP1A1 and CYP1B1 by TS is consistent with evidence that the AhR plays a central role in regulating these genes. The AhR had been linked to carcinogenesis (47, 48), and the polycyclic aromatic hydrocarbons in TS bind to and activate the AhR, resulting in the induction of CYP1A1 and CYP1B1 (13, 38, 41). Following ligand-induced activation by polycyclic aromatic hydrocarbons, the AhR releases its chaperoning heat shock protein 90, translocates into the nucleus, and dimerizes with ARNT (49). The heterodimer binds to xenobiotic response elements present in the 5' flanking region of target genes and thereby modulates transcription. In addition to CYP1A1 and CYP1B1, polycyclic aromatic hydrocarbons induce the phase II xenobiotic metabolizing enzyme NAD(P)H:quinone oxidoreductase (NQO1) and the AhR repressor. The AhR and AhR repressor are believed to constitute a negative feedback loop of xenobiotic signal transduction. The liganded AhR induces AhR repressor transcription, whereas expressed AhR repressor, in turn, inhibits the function of AhR (49). Both NQO1 and AhR repressor were induced in the TS-treated MSK-Leuk1 cells although the magnitude of this induction was less than for CYP1A1 and CYP1B1. Clearly, these results suggest that it will be worthwhile to determine if increased levels of NQO1 and AhR repressor also occur in the buccal mucosa of smokers. Easily accessible buccal mucosa may serve as a surrogate tissue for understanding the effects of TS on the biology of difficult-to-obtain bronchial mucosa. In support of this notion, we found that TS induced changes in the transcriptome of MSK-Leuk1 cells that were mimicked by differences in bronchial mucosa of smokers versus nonsmokers. The AhR-driven gene induction observed in the MSK-Leuk1 model matches the *in vivo* results in the airway epithelial cells of smokers (Table 3). In this regard, the fact that a small subset (CYP1A1 and CYP1B1) of highly inducible genes was also overexpressed in the buccal mucosa of smokers is of interest. Future studies of the transcriptome of buccal mucosa of smokers versus never smokers will be needed to draw more definitive conclusions about how closely the biology of the buccal mucosa reflects changes in the lower respiratory tract.

Our pathway analysis showed that treatment of MSK-Leuk1 cells altered the expression of genes involved in cellular proliferation, raising the possibility that TS amplifies its own mutagenicity by stimulating the proliferation of cells because conversion of TS-induced DNA adducts to mutations can only occur in proliferating cells (50). Enhanced cell proliferation has been observed in the aerodigestive tracts of active smokers (51). Interestingly, intracellular levels of glutathione, an antioxidant, have been shown to modulate the effects of TS condensate on cell proliferation (52). Notably, we find that the glutathione metabolism pathway is induced both in MSK-Leuk1 cells and in the airway epithelial cells of smokers.

We and others found that TS-mediated activation of EGFR signaling led to increased cell proliferation (36, 37). In the current study, treatment with TS led to increased levels of both EGFR and its ligands including AREG, TGFA, HB-EGF, and EREG, forming an EGFR-centered hub within the interactome maps. Collectively, these findings strengthen the rationale for evaluating whether an inhibitor of EGFR tyrosine kinase can prevent or delay the onset of TS-related malignancies of the aerodigestive tract.

Our pathway analysis suggests that TS modulates cell movement, apoptosis, immune function, and coagulation. Both inflammation and immune suppression have been suggested to contribute to TS-induced carcinogenesis (53). Consistently, we identified the differential expression of several interleukins and their receptors, including IL1A, IL1B, IL1RN, IL1R1, IL1R2, IL6, IL7R, IL8, IL11, IL17RC, IL20, and IL24, in addition to TNFA, where IL1B, IL1R1, IL1RN, and IL8 are connected within a network. Our pathway-level analysis also links TS exposure to the induction of specific inflammatory pathways (Table 2).

Taken together, our results provide new insights into the potential mechanisms underlying procarcinogenic effects of TS and may help to explain the worse outcome of cancer patients who continue to smoke. Furthermore, our results suggest important targets for future studies designed to identify agents that could reduce or eliminate the detrimental effects of TS exposure indicated by the findings presented here.

Disclosure of Potential Conflicts of Interest

No potential conflicts of interest were disclosed.

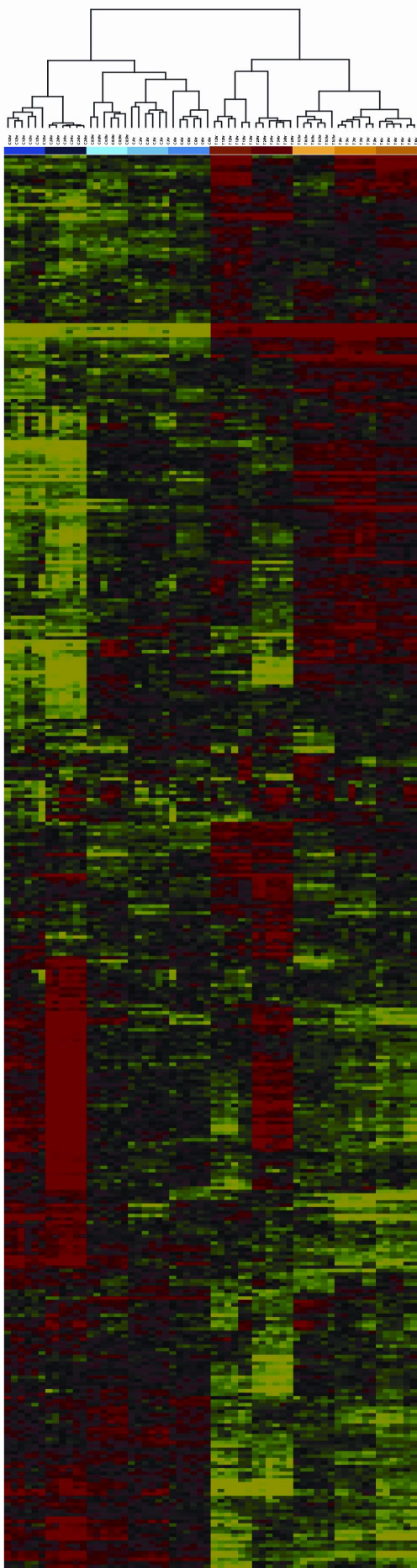
Acknowledgments

We thank Jenny Xiang from the Microarray Core of Weill Cornell Medical College for expert help and Kevin C. Dorff from the Institute for Computational Biomedicine for webpage design.

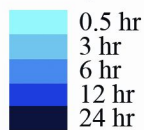
References

- Gritz ER, Dresler C, Sarna L. Smoking, the missing drug interaction in clinical trials: ignoring the obvious. *Cancer Epidemiol Biomarkers Prev* 2005; 14:2287-93.
- Tobacco smoke and involuntary smoking. *IARC Monogr Eval Carcinog Risks Hum* 2004;83:1-1438.
- Hecht SS. Tobacco carcinogens, their biomarkers and tobacco-induced cancer. *Nat Rev Cancer* 2003;3:733-44.
- Mayne ST, Lippman SM. Cigarettes: a smoking gun in cancer chemoprevention. *J Natl Cancer Inst* 2005;97:1319-21.
- The α -Tocopherol, β Carotene Cancer Prevention Study Group. The effect of vitamin E and β carotene on the incidence of lung cancer and other cancers in male smokers. *N Engl J Med* 1994;330:1029-35.
- Hamilton M, Wolf JL, Rusk J, et al. Effects of smoking on the pharmacokinetics of erlotinib. *Clin Cancer Res* 2006;12:2166-71.
- Khuri FR, Lee JJ, Lippman SM, et al. Randomized phase III trial of low-dose isotretinoin for prevention of second primary tumors in stage I and II head and neck cancer patients. *J Natl Cancer Inst* 2006;98:441-50.
- Fox JL, Rosenzweig KE, Ostroff JS. The effect of smoking status on survival following radiation therapy for non-small cell lung cancer. *Lung Cancer* 2004;44:287-93.
- Pantarotto J, Malone S, Dahrouge S, Gallant V, Eapen L. Smoking is associated with worse outcomes in patients with prostate cancer treated by radical radiotherapy. *BJU Int* 2007;99:564-9.
- Shepherd FA, Rodrigues Pereira J, Ciuleanu T, et al. Erlotinib in previously treated non-small-cell lung cancer. *N Engl J Med* 2005;353:123-32.

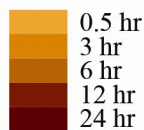
11. Browman GP, Wong G, Hodson I, et al. Influence of cigarette smoking on the efficacy of radiation therapy in head and neck cancer. *N Engl J Med* 1993;328:159–63.
12. Guengerich FP, Shimada T. Activation of procarcinogens by human cytochrome P450 enzymes. *Mutat Res* 1998;400:201–13.
13. Murray GI, Melvin WT, Greenlee WF, Burke MD. Regulation, function, and tissue-specific expression of cytochrome P450 CYP1B1. *Annu Rev Pharmacol Toxicol* 2001;41:297–316.
14. Ko Y, Abel J, Harth V, et al. Association of CYP1B1 codon 432 mutant allele in head and neck squamous cell cancer is reflected by somatic mutations of p53 in tumor tissue. *Cancer Res* 2001;61:4398–404.
15. Spira A, Beane J, Shah V, et al. Effects of cigarette smoke on the human airway epithelial cell transcriptome. *Proc Natl Acad Sci U S A* 2004;101:10143–8.
16. Sacks PG. Cell, tissue and organ culture as *in vitro* models to study the biology of squamous cell carcinomas of the head and neck. *Cancer Metastasis Rev* 1996;15:27–51.
17. Moraitis D, Du B, De Lorenzo MS, et al. Levels of cyclooxygenase-2 are increased in the oral mucosa of smokers: evidence for the role of epidermal growth factor receptor and its ligands. *Cancer Res* 2005;65:664–70.
18. Choe SE, Boutros M, Michelson AM, Church GM, Halfon MS. Preferred analysis methods for Affymetrix GeneChips revealed by a wholly defined control data set. *Genome Biol* 2005;6:R16.
19. Irizarry RA, Bolstad BM, Collin F, et al. Summaries of Affymetrix GeneChip probe level data. *Nucleic Acids Res* 2003;31:e15.
20. Wu Z, Irizarry RA, Gentleman RFM, Spencer F. A model based background adjustment for oligonucleotide expression arrays. *J Am Stat Assoc* 2003;99:909–17.
21. Shedden K, Chen W, Kuick R, et al. Comparison of seven methods for producing Affymetrix expression scores based on false discovery rates in disease profiling data. *BMC Bioinformatics* 2005;6:26.
22. Cope LM, Irizarry RA, Jaffee HA, Wu Z, Speed TP. A benchmark for Affymetrix GeneChip expression measures. *Bioinformatics* 2004;20:323–31.
23. Millenaar FF, Okyere J, May ST, et al. How to decide? Different methods of calculating gene expression from short oligonucleotide array data will give different results. *BMC Bioinformatics* 2006;7:137.
24. Allison DB, Cui X, Page GP, Sabripour M. Microarray data analysis: from disarray to consolidation and consensus. *Nat Rev Genet* 2006;7:55–65.
25. Benjamini Y, Hochberg Y. Controlling the false discovery rate: a practical and powerful approach to multiple testing. *J R Stat Soc B Met* 1995;57:289–300.
26. Tusher VG, Tibshirani R, Chu G. Significance analysis of microarrays applied to the ionizing radiation response. *Proc Natl Acad Sci U S A* 2001;98:5116–21.
27. Subramanian A, Tamayo P, Mootha VK, et al. Gene set enrichment analysis: a knowledge-based approach for interpreting genome-wide expression profiles. *Proc Natl Acad Sci U S A* 2005;102:15545–50.
28. Rhodes DR, Tomlins SA, Varambally S, et al. Probabilistic model of the human protein-protein interaction network. *Nat Biotechnol* 2005;23:951–9.
29. Available from: <http://www.ingenuity.com> [cited 2007 Dec 15].
30. Hosack DA, Dennis G, Sherman BT, Lane HC, Lempicki RA. Identifying biological themes within lists of genes with EASE. *Genome Biol* 2003;4:R70.
31. Tomfohr J, Lu J, Kepler TB. Pathway level analysis of gene expression using singular value decomposition. *BMC Bioinformatics* 2005;6:225.
32. Barry WT, Nobel AB, Wright FA. Significance analysis of functional categories in gene expression studies: a structured permutation approach. *Bioinformatics* 2005;21:1943–9.
33. Eisen MB, Spellman PT, Brown PO, Botstein D. Cluster analysis and display of genome-wide expression patterns. *Proc Natl Acad Sci U S A* 1998;95:14863–8.
34. Ma P, Castillo-Davis CI, Zhong W, Liu JS. A data-driven clustering method for time course gene expression data. *Nucleic Acids Res* 2006;34:1261–9.
35. Tan MP, Broach JR, Floudas CA. A novel clustering approach and prediction of optimal number of clusters: I. Global optimum search with enhanced positioning. *J Global Optimization* 2007;39:323–46.
36. Du B, Altorki NK, Kopelovich L, Subbaramaiah K, Dannenberg AJ. Tobacco smoke stimulates the transcription of amphiregulin in human oral epithelial cells: evidence of a cyclic AMP-responsive element binding protein-dependent mechanism. *Cancer Res* 2005;65:5982–8.
37. Lemjabbar H, Li D, Gallup M, et al. Tobacco smoke-induced lung cell proliferation mediated by tumor necrosis factor α -converting enzyme and amphiregulin. *J Biol Chem* 2003;278:26202–7.
38. Port JL, Yamaguchi K, Du B, et al. Tobacco smoke induces CYP1B1 in the aerodigestive tract. *Carcinogenesis* 2004;25:2275–81.
39. Du B, Leung H, Khan KM, et al. Tobacco smoke induces urokinase-type plasminogen activator and cell invasiveness: evidence for an epidermal growth factor receptor dependent mechanism. *Cancer Res* 2007;67:8966–72.
40. Peri S, Navarro JD, Amanchy R, et al. Development of human protein reference database as an initial platform for approaching systems biology in humans. *Genome Res* 2003;13:2363–71.
41. Brauze D, Widerak M, Cwykiel J, Szyfter K, Baer-Dubowska W. The effect of aryl hydrocarbon receptor ligands on the expression of AhR, AhRR, ARNT, Hif1 α , CYP1A1 and NQO1 genes in rat liver. *Toxicol Lett* 2006;167:212–20.
42. Spivack SD, Hurteau GJ, Jain R, et al. Gene-environment interaction signatures by quantitative mRNA profiling in exfoliated buccal mucosal cells. *Cancer Res* 2004;64:6805–13.
43. Josephy PD, Batty SM, Boverhof DR. Recombinant human P450 forms 1A1, 1A2, and 1B1 catalyze the bioactivation of heterocyclic amine mutagens in *Escherichia coli* lacZ strains. *Environ Mol Mutagen* 2001;38:12–8.
44. Shimada T, Hayes CL, Yamazaki H, et al. Activation of chemically diverse procarcinogens by human cytochrome P-450 1B1. *Cancer Res* 1996;56:2979–84.
45. Denissenko MF, Pao A, Tang M, Pfeifer GP. Preferential formation of benzo[a]pyrene adducts at lung cancer mutational hotspots in P53. *Science* 1996;274:430–2.
46. McFadyen MC, McLeod HL, Jackson FC, et al. Cytochrome P450 CYP1B1 protein expression: a novel mechanism of anticancer drug resistance. *Biochem Pharmacol* 2001;62:207–12.
47. Shimizu Y, Nakatsuru Y, Ichinose M, et al. Benzo[a]pyrene carcinogenicity is lost in mice lacking the aryl hydrocarbon receptor. *Proc Natl Acad Sci U S A* 2000;97:779–82.
48. Andersson P, McGuire J, Rubio C, et al. A constitutively active dioxin/aryl hydrocarbon receptor induces stomach tumors. *Proc Natl Acad Sci U S A* 2002;99:9990–5.
49. Mimura J, Fujii-Kuriyama Y. Functional role of AhR in the expression of toxic effects by TCDD. *Biochim Biophys Acta* 2003;1619:263–8.
50. Cohen SM, Ellwein LB. Cell proliferation in carcinogenesis. *Science* 1990;249:1007–11.
51. van Oijen MG, Gilsing MM, Rijkse G, Hordijk GJ, Slootweg PJ. Increased number of proliferating cells in oral epithelium from smokers and ex-smokers. *Oral Oncol* 1998;34:297–303.
52. Luppi F, Aarbiou J, vanWetering S, et al. Effects of cigarette smoke condensate on proliferation and wound closure of bronchial epithelial cells *in vitro*: role of glutathione. *Respir Res* 2005;6:140.
53. Ballaz S, Mulshine JL. The potential contributions of chronic inflammation to lung carcinogenesis. *Clin Lung Cancer* 2003;5:46–62.



C



TS



Supplementary Figure 1:

Hierarchical clustering using 411 probesets differentially expressed in MSK-Leuk1 cells treated with tobacco smoke condensate (TS) and vehicle treated controls (C) at 0.5, 3, 6, 12 and 24 hr time points. In this heatmap, red signifies high levels of expression; green, low levels of expression and black, mean level of expression.